Research Article

EFFECT OF THE ACID HYDROLYSIS CONDITIONS ON THE FUNCTIONAL PROPERTIES OF MICROCRYSTALLINE CELLULOSE II

John Rojas[1]*, Luisa Ospina, Sandra Fonseca
[1]Department of Pharmacy, School of Pharmaceutical Chemistry, The University of Antioquia, Medellín, Columbia.
*Corresponding author's E-mail: jrojasca@gmail.com

Accepted on: 15-12-2011; **Finalized on:** 20-02-2012.

ABSTRACT

Microcrystalline cellulose II (MCCII) was prepared from wood cotton. Hydrolysis conditions were performed according to the Box Benhken design composed of three factors: acid type (hydrochloric, sulfuric and nitric acids), acid concentration (1, 3 and 5 M) and reaction time (3, 4 and 5 h). Hydrolysis conditions only affected particle size, flow rate, degree of polymerization and dissolution rate of spironolactone. However, only the effect of hydrolysis on particle size and flow rate was considered as significant. The quadratic model determined hydrolysis with 2.2 M HCl or H_2SO_4 for 3h and as the optimal reaction conditions to produce a MCCII with a particle size of ~100 µm and flow rate of ~20 g/sec. The validation runs gave particle size and flow rate values of 112 µm and 24.3 g/sec and 96 µm and 17.2 g/sec when hydrochloric and sulfuric acids were employed, respectively. Further, compacts made of MCCII and spironolactone (a poorly soluble drug) released at least 80% of the drug between 18-34 min, independent of the hydrolysis conditions employed.

Keywords: Microcrystalline cellulose II, acid hydrolysis, wood and surgical cotton.

INTRODUCTION

Cotton has been widely used in the textile, dental and pharmaceutical fields for the manufacture of fabrics, sorption of biological fluids and hygiene purposes. In the manufacture of cotton, especially that intended for pharmaceutical and dental applications, a great amount of residues are generated that can be used to produce excipients. Since more than 95% of cotton is composed of α-cellulose. It can be used to produce microcrystalline cellulose I (MCCI) and its derivatives[1].

Traditionally, microcrystalline cellulose I MCCI has been the leading excipient for the production of solid dosage forms. It is available in various particle size grades and used in direct compression and wet granulation processes[2]. It is commonly produced by acid treatment of native cellulose to hydrolyze the more accessible amorphous regions until the limiting degree of polymerization is reached[3,4]. During the acid hydrolysis recrystallization in some of the defective crystallites and degradation of the disordered areas of cellulose occur simultaneously[5]. The resulting slurry is neutralized, tray-dried or spray-dried to obtain a powder.

The source or origin of cellulose might affect the fundamental and derived properties of this material. For example, the mechanical properties of MCCI from hardwood are better than those shown by powders obtained from softwood[6]. Further, yield of MCCI is also dependant on the cellulose source. MCCI obtained from cotton linters usually have yields higher than 95%[7]. Likewise, different commercial grades of MCCI may differ in particle size, physical form and in the ratio of well-ordered crystalline to amorphous regions, causing inter lot or brand variability, respectively. It has been reported considerable variability in the MCCI properties, having all compliance with the compendial specifications[8-10]. For instance, Avicel® and Emcocel® products have the most similarities based on tableting indices. However, a significant lot-to-lot variation has been observed for Fibrocel®, Omnicel®, and Spectrum® MCCI products. The improved ease of processing with Avicel® and Emcocel® may be related to its small particle size with improved flow, and low depolymerization[11].

Different cellulose sources like viscose staple, bagasse, ramie and cotton after acid treatment might show changes in crystallinity, particle size distribution and morphological features of the particles. However, crystallinity does not have any effect on the mechanical properties of the resulting MCCI tablets[8]. Furthermore, sulfuric acid is known to render whisker/crystallites of cellulose which are easy to redisperse in water[9]. Further, hydrolysis of MCCI with sulfuric and hydrochloric acids influences the crystallite size and degree of polymerization showing a larger degree of polymerization when Hydrochloric acid was employed[12,13]. The same study reported no significant effects due to the acid hydrolysis on the bulk and tap densities, whereas particle size was affected especially when sulfuric acid was employed which rendered high particle size and smaller surface area[14]. MCCI hydrolyzed with sulfuric acid rendered compacts with better mechanical properties than powders produced with Hydrochloric acid [15].

The microcrystalline cellulose (MCCII) allomorph was recently introduced as a new filler/binder for solid dosage forms, and has been recommended as a suitable excipient when a rapidly disintegrating compact is desirable[16,17]. It has a higher bulk and tap densities than MCCI. Further, MCCII also has lower porosity, true density, plasticity and

compactibility than MCCI. These results suggest the polymorphic form, rather than the cellulose source or the process employed as the cause of these changes.

The aim of this study was to evaluate the influence of acid hydrolysis conditions such as type of acid, its concentration and hydrolysis time on the powder and tableting properties of MCCII by using a Box Behnken experimental design.

MATERIALS AND METHODS

Materials

Sodium hydroxide (lot 1105009-2), concentrated sulfuric acid (97% w/v, lot L1104042-1), concentrated hydrochloric acid (37%, lot 1101036) and nitric acid (70% w/v, lot 1105057-2) were purchased from Protokimica (Medellin, Columbia). Wood cotton was obtained from New Stetics Laboratories (Medellin, Columbia). Spironolactone (lot MPO33H-10) was donated by Humax Pharmaceutica SA (Medellin, Columbia). Sodium Lauryl Sulfate (lot 984881) was obtained from Fisher Scientific (Fair Lawn, NJ).

Preparation of cellulose II

Approximately 5 kg of wood cotton was soaked in 40 L of a 7.5 N solution of sodium hydroxide at room temperature with periodic stirring. After 72 h the resulting fibers were filtered and washed with distilled water until reaching a pH from 5 to 7.

Preparation of microcrystalline cellulose II (MCCII)

Approximately, 280 g of cellulose II fibers were added to a round bottom flask containing ~2600 mL of acid and hydrolyzed at 100 ºC at the corresponding conditions shown in Table 1 using a heating mantle (P & P, MC-4000, Medellín, Columbia). The wet mass thus obtained was then washed with distilled water until reaching a pH from 5 to 7, and conductivity < 20 µS/cm. The resulting materials were dried on a convection oven (model STM 80, Rigor Scientific, Inc., Chicago, IL, USA) at 60ºC until reaching a moisture content of ~45% and granulated using a Riddi oscillating granulator (Riddhi Pharma Machinery, Gulabnagar, India), equipped with a 710 µm screen. The granulation step was then repeated at 30% and 20% moisture contents using screens having an aperture of 420 µm and 150 µm, respectively. The resulting powder was dried at 60ºC until reaching a moisture content < 5%.

FT-IR characterization

Approximately, 1 mg of sample was mixed with 100 mg of KBr (both previously dried at 110°C for 4 h before used) on an agate mortar and pestle. Pellets of these mixtures were then made on a portable press at a dwell time of 5 min and at a force of 10,000 pounds. The infrared spectra were collected between 650 and 4000 cm^{-1} on a Perkin Elmer IR Spectrometer (Spectrum BX, PerKin Elmer, CA, USA) equipped with the Ommic software (Nicolet Corp., Madison, WI, USA). The resolution, interval length, and number of scans employed were 16, 2, and 16 cm^{-1}, respectively.

Box Behnken experimental design for MCCII

A Box Behnken surface response design composed of 15 runs (Table 1), 3 factors (acid type, acid concentration and hydrolysis time) and 3 levels (Table 2) was employed to assess the effects of these hydrolysis conditions on the resulting functional properties of MCCII. The software Minitab (v.16, Minitab®, Inc., State College, PA) was used for the statistical analysis.

Table 1: Box Behnken Experimental matrix for MCC II

Run	Acid	Acid concentration (M)	Hydrolysis Time (h)
1	HNO_3	3	3
2	HCl	3	3
3	HCl	5	4
4	H_2SO_4	1	3
5	H_2SO_4	3	4
6	HNO_3	5	4
7	H_2SO_4	1	5
8	H_2SO_4	5	5
9	H_2SO_4	5	3
10	HNO_3	3	5
11	HCl	3	5
12	H_2SO_4	3	4
13	H_2SO_4	3	4
14	HNO_3	1	4
15	HCl	1	4

Table 2: Independent variables of the Box Behnken design and their respective levels

Acid type	Acid concentration (M)	Hydrolysis time (h)
HCl	1	3
H_2SO_4	3	4
HNO_3	5	5

Powder X-ray diffraction characterization

Powder X-ray diffractions were conducted over a 5-45° 2θ range using a Rigaku Bench top diffractometer (Miniflex II, Rigaku Americas, The woodlands, TX, USA) at 40 kV and 30 mA, equipped with a monochromatic CuKα (α_1 = 1.5418 Å, α_2 = 1.5444 Å) X-ray radiation. The step width was 0.020° 2θ/min with a time constant of 0.5 sec.

Powder properties

Optical microphotographs were taken on an optical microscope (BM-180, Boeco, Germany) coupled with a digital camera (S8000fd, Fujifilm Corp., Japan) at a 10X magnification. Moisture content was obtained by gravimetry on ~5 g of sample dried on a convection oven (STM 80, Rigor Scientific, Inc., Chicago, IL). The powder true density was determined on a helium picnometer (AccuPyc II 1340, Micromeritics, U.S.A.) with ~2 g of

sample. Bulk density was determined by the ratio of 20 g of sample divided by the measured volume on a 100 mL graduated cylinder. Flow rate was obtained by measuring the time for ~20 g of sample to pass through a glass funnel (63.7 mm dia.).

Degree of polymerization (DP)

It was obtained by the intrinsic viscosity method [η] at 25 ± 0.5°C using a Cannon-Fenske capillary viscometer (cell size 50) and Cupriethylendiamine hydroxide (CUEN) as solvent[18]. The DP was found by the relationship:

$$DP=[\eta]*190 \qquad \text{Eqn. 1}$$

Where DP and [η] correspond to the degree of polymerization and intrinsic viscosity, respectively

Particle size

Samples were fractionated on a RO-TAP sieve shaker (RX29, W.S. Tyler Co., Mentor, OH, U.S.A.) using a stainless steel 38, 45, 53, 75, 106, 125 and 150 µm sieves, stacked together in the order written (Fisher Scientific Co., Pittsburgh, PA, U.S.A.). Approximately 25 g of sample was shaken for 30 min followed by weighing the fractions retained in each sieve. The geometric mean diameter (dg) was determined from the log-normal distribution plot constructed between the sieve mean diameter and cumulative percent frequency using the Minitab software (v.16, Minitab, Inc., State College, PA, U.S.A.).

Preparation of compacts

A mixture of 20% spironolactone and 80% MCCII was prepared on a twin shell blender (Riddhi Pharma Machinery, Gulabnagar, India) for 15 min. Cylindrical compacts of ~500 mg were made on a single punch tablet press (Compac 060804, Indemec Ltda., Itagüí, Columbia) coupled with a 13 mm flat-faced tooling. The compression force was adjusted so the resulting compacts had a solid fraction between 0.85-0.90.

Disintegration time

The USP32/NP27 method was employed. Briefly, a Hanson disintegrator (39-133-115, Hanson Research Corporation, Northridge, CA, U.S.A.) was used with water maintained at 37 ± 5°C and 30 strokes/min[19].

Compact tensile strength

It was determined on a Stokes hardness tester (UK 200, VANKEL, Manasquan, NJ, U.S.A.). Each compact was placed between the platens and the crushing force was then measured. The radial tensile strength (TS) values were obtained according to the Fell and Newton equation as reported previously[20].

Spironolactone dissolution

It was conducted on a Vankel (VK 7000, Palo Alto, CA, USA) dissolution apparatus 2 with paddles (Scientific Instruments and Technology Corp., Piscataway, NJ) in 0.1 N HCl containing 0.1% sodium lauryl sulfate at 37°C and at a stirring speed of 75 rpm for 1h. At 5, 10, 15, 30, 45 and 60 min, aliquots (1 mL each) of the dissolution medium were withdrawn, passed through a 0.22 µm membrane filter and analyzed for spironolactone content. The removed dissolution medium was replaced with an equal volume of dissolution media. Aliquots were analyzed by UV-VIS spectrophotometry (Shimadzu UV-240, Kyoto, Japan) at 242 nm. Drug content was obtained by interpolation from a spironolactone calibration curve prepared at 5, 10 and 25 µg/mL concentrations.

RESULTS AND DISCUSSION

Figure 1 shows the powder X-ray diffractograms of wood cotton containing the cellulose I lattice and cellulose II respectively. The diffraction peaks appearing at 12, 20, and 22° 2θ which occurred after the alkaline treatment of wood cotton with NaOH confirmed the cellulose II lattice attributable to 1 ī 0, 110 and 200 reflections, respectively[21]. Non-treated wood cotton, in contrast, displayed characteristic diffraction peaks at 14.8, 16.3 and 22.4° 2θ, corresponding to the 1 ī 0, 110 and 200 reflections of cellulose I, respectively[22].

The FT-IR spectra of MCCII after conducting hydrolysis at the conditions shown in Table 1 are shown in Figure 2. The different hydrolysis conditions did not change the vibrational bands typical of cellulose. These characteristic vibrational peaks are present at ~3446 cm^{-1}, 2899 cm^{-1}, 1379 cm^{-1} and 893 cm^{-1}, attributable to intramolecular OH stretching, CH stretching, hydrogen bonding between C6 and its OH group, and antisymmetric C-1 out-of-plane stretching vibrations, respectively. The 893 cm^{-1} band has also been reported to be associated with the cellulose II lattice and its crystallinity[23].

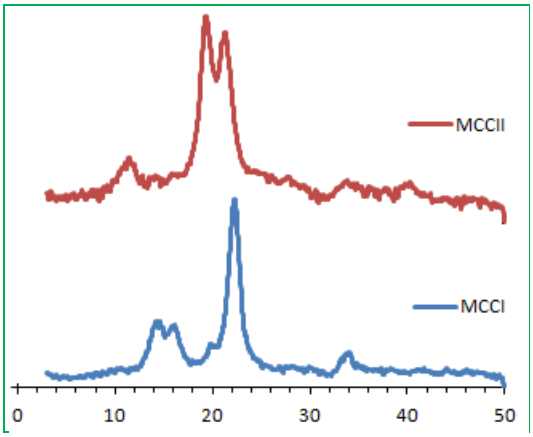

Figure 1: XRD of cellulose I from wood cotton and cellulose II obtained after its alkaline treatment.

Figure 3 depicts typical microphotographs of MCCII obtained from the three mineral acids selected in this study. Hydrochloric acid rendered small particles forming irregular aggregates. Nitric acid, on the other hand, rendered elongated fibers with no aggregates. Sulfuric acid rendered particles with aggregates in a lower degree compared to those of hydrochloric acid.

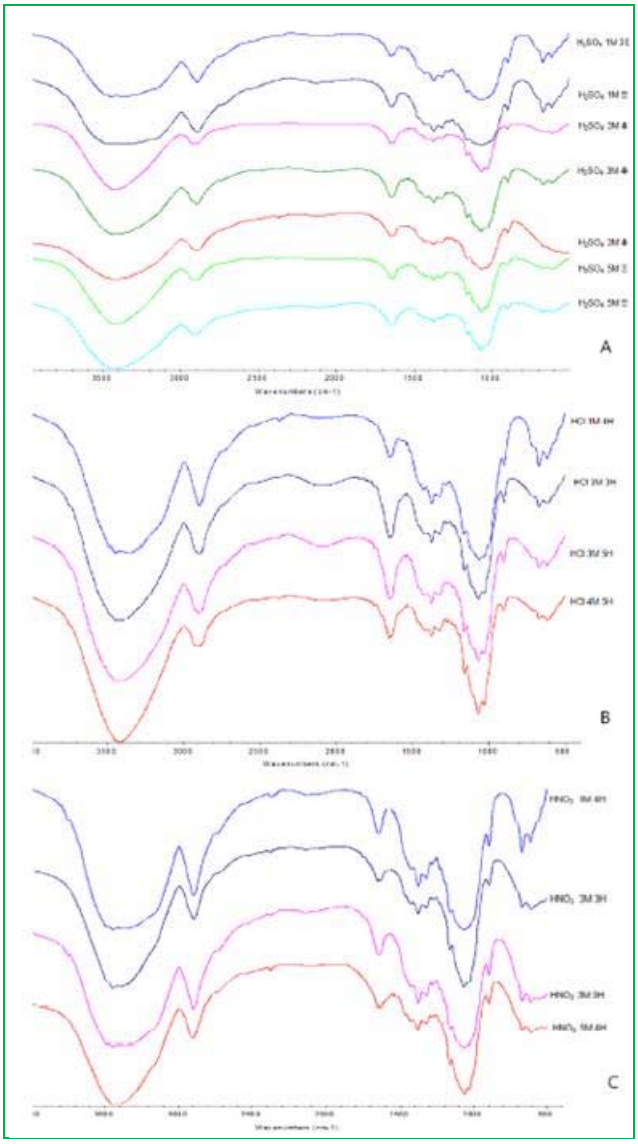

Figure 2: FT-IR Spectra of MCCII treated under different hydrolysis conditions: A, HCl; B. H_2SO_4; C, HNO_3.

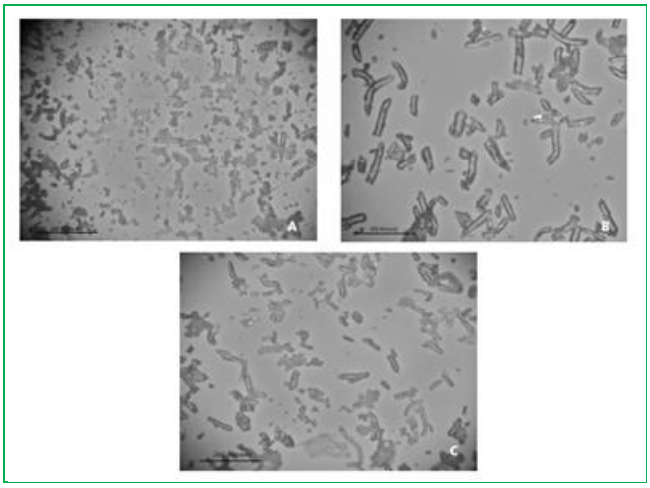

Figure 3: Selected Microphotographs of MCCII obtained after treatment with: A, HCl, B, HNO_3; H_2SO_4

Table 3 lists the selected properties of MCCII obtained from the hydrolysis conditions listed in Table 1. Particle size seems to be highly affected by the acid type (p= 0.005) used independent of the concentration and time employed. In this case, materials treated with nitric acid seem to have a smaller particle size than those treated with HCl and HNO_3. This behavior is unusual since a small particle size was only expected for the stronger diprotic sulfuric acid. In this case, it is possible that cellulose was more susceptible to a reduction in particle size due to the faster elimination of amorphous regions due to hydrolysis with nitric acid.

Further, the degree of polymerization had not relationship with the acid type employed. However, if the product of particle size expressed as geometric mean (D_g) and bulk density (ρ_{bulk}) is plot against degree of polymerization, a fairly linear relationship is obtained. This indicates that products which had low values of $Dg^*\rho_{bulk}$ also had low degrees of polymerization (Fig. 4).

Table 3: Powder properties of MCCII obtained at different hydrolysis conditions.

Hydrolisis condition	Dg (µm)	True density (g/ cm^3)	Bulk density (g/ cm^3)	Porosity	Flow rate (g/sec)	MC (%)	DP
	n=1	n=3	n=3	n=1	n=3	n=1	n=1
HCl 3M 5h	102.5 (27)	1.535 (0.00)	0.50 (0.00)	0.67	14.62	4.2	126.3
HNO_3 3M 3h	53.2 (13.2)	1.54 (0.00)	0.59 (0.02)	0.62	7.32	3.2	85.4
HCl 5M 4h	128.9 (12.9)	1.60(0.00)	0.59 (0.02)	0.63	19.88	4.5	77.9
HNO_3 5M h	29.9 (3.9)	1.52(0.00)	0.52 (0.02)	0.66	5.25	5.1	68
H_2SO_4 1M 3h	58.6 (13.8)	1.50(0.00)	0.57 (0.0)	0.62	17.81	2.9	108.2
HCl 3M 3h	130 (13.1)	1.50(0.00)	0.61 (0.01)	0.59	18.80	4.4	98
H_2SO_4 3M 4h	116.8 (18.3)	1.50(0.00)	0.65 (0.01)	0.57	17.86	5.0	101.1
H_2SO_4 3M 4h	128.4 (17.3)	1.59(0.00)	0.55 (0.02)	0.65	18.90	3.6	113.9
H_2SO_4 3M 4h	89.9 (21.1)	1.58(0.00)	0.5 (0.0)	0.68	17.42	4.4	107.6
HNO_3 1M 4h	23.3 (1.7)	1.56 (0.00)	0.43 (0.02)	0.72	8.46	3.4	95.3
H_2SO_4 1M 5h	115.2 (19.7)	1.54 (0.00)	0.61 (0.02)	0.60	11.57	2.7	72.8
HCl 1M 4h	41.6 (8.1)	1.53(0.00)	0.57 (0.02)	0.63	8.92	4.8	110.2
H_2SO_4 5M 5h	108.1 (16.7)	1.56(0.00)	0.60 (0.02)	0.62	17.13	3.0	111.6
H_2SO_4 5M 3h	109.2 (20)	1.60(0.00)	0.56 (0.05)	0.65	10.50	3.6	128.2
HNO_3 3M 5h	41.3 (8.1)	1.54 (0.00)	0.58 (0.01)	0.62	6.65	4.3	101.6
p-value	0.005	0.718	0.416	0.053	0.004	0.440	0.256

Dg, particle size expressed as geometric mean; MC, moisture content; DP, degree of polymerization

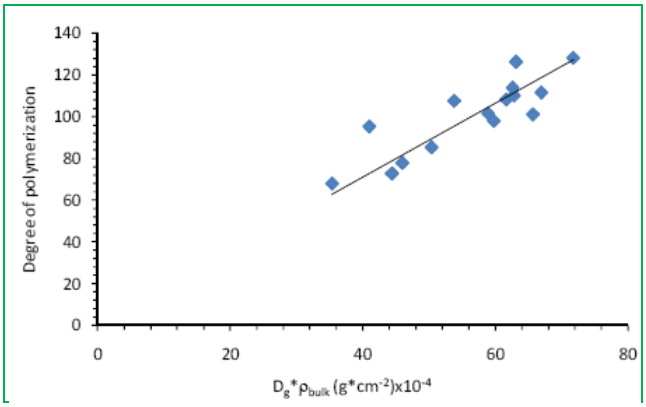

Figure 4: Effect of particle size and bulk density on the degree of polymerization of MCCII.

In other words, a material with a low particle size and density had a low average polymer length and hence, molecular weight. Conversely, the true density of these materials had no relationship with the hydrolysis conditions employed and ranged from 1.5 to 1.61 g/cc. Moreover, bulk density alone had not relationship with flow rate. Therefore, it is possible that several factors, such as morphology, along with powder density and particle size altogether influenced flow. On the contrary, the effect of moisture content on the above properties is considered negligible since in all cases it was lower than 5%. Powder porosity as expected was inversely correlated to bulk density. The p-values obtained only determined particle size and flow rate as significant for the type of acid employed (*p values* of 0.005 and 0.004, respectively) since none of the properties were significant for time and acid concentration.

Figure 5 depicts the surface plots for particle size of MCCII. Hydrochloric and sulfuric acids rendered MCCII with the largest particle sizes (> 60 µm), whereas nitric acid produced the smallest sizes (< 60 µm). Further, all the surface plots exhibited a slide shape independent of the acid employed. Hydrolysis time had smaller effect on particle size than acid concentration. This indicates that the reduction of long fibers of cotton occurred within the first three hours of hydrolysis and then the reduction was accelerated. This small reduction of particle size with time (3-5 h) could be attributed to the low amount of hydrogen ion available for cutting the β-1-4 glycosidic linkage between glucose present in the amorphous regions of cellulose fibers making those particles shorter with increasing hydrolysis time. On the contrary, high acid concentrations favored particle size possibly due to the large amount of small size porous fibers produced which upon granulation were more prompt to form aggregates of larger sizes.

Figure 6 shows the flow rate surface plots of MCCII as a function of time and concentration. Independent of the acid type employed for hydrolysis, long hydrolysis times decreased flow rate at low concentrations, but at high concentration and times, flow rate is favored. The latter case is ascribed to the combined effect of increased bulk density and low powder porosity in the resulting particles, due to the more effective formation of larger particles and aggregates.

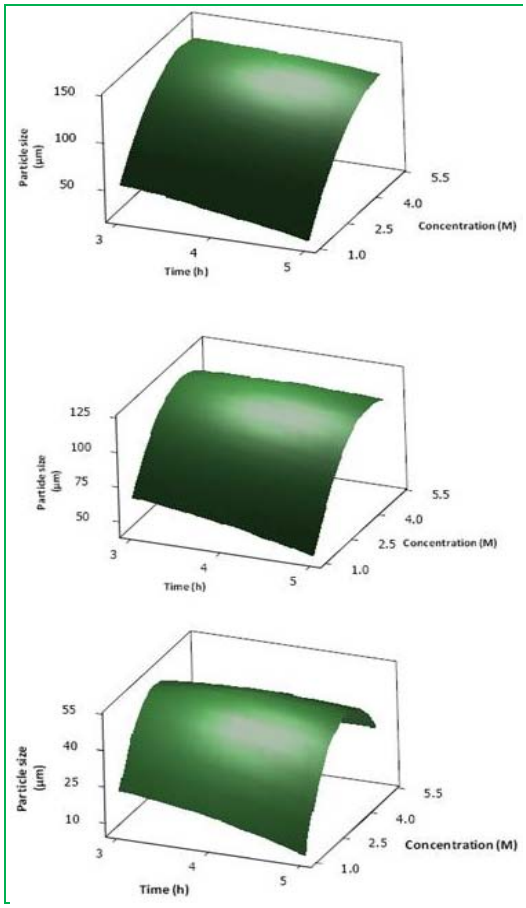

Figure 5: Surface plots for Particle size vs. time and concentration of MCCII after treatment with: a, HCl; b, H_2SO_4; c, HNO_3.

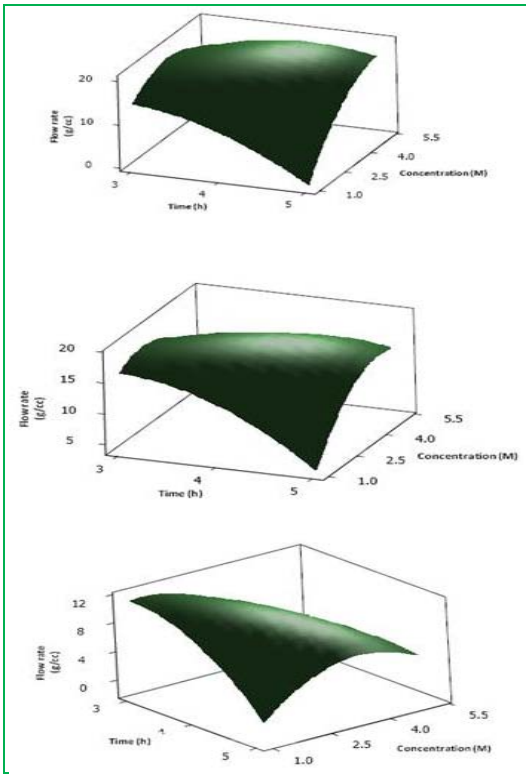

Figure 6: Surface plots for flow rate vs. time and concentration for: a, HCl; b, H_2SO_4; c, HNO_3.

Table 4: Regression coefficients of the square models for particle size and flow rate of MCCII.

Term	Coeff.	SE Coeff.	t value	p-value
Constant	-46.2	143.9	-0.32	0.761
Acid (A)	93.6	45.5	2.06	0.095
Time (T)	-4.5	63.4	-0.07	0.946
Concentration (C)	64.7	20.1	3.23	0.023
A*A	-27.7	8.3	-3.36	0.020
T*T	-2.2	8.3	-0.27	0.798
C*C	-7.0	2.1	-3.4	0.019
A*T	3.9	7.2	0.54	0.613
A*C	-10.1	3.6	-2.79	0.039
T*C	2.8	4.9	-0.56	0.598
Constant	-11.3	22.6	-0.50	0.638
Acid (A)	11.7	7.2	1.64	0.162
Time (T)	11.3	9.9	1.13	0.310
Concentration (C)	1.6	3.2	0.50	0.636
A*A	-3.6	1.3	-2.75	0.040
T*T	-2.7	1.3	-2.05	0.096
C*C	-1.0	0.3	-2.99	0.031
A*T	0.9	1.2	0.77	0.475
A*C	-1.8	0.6	-3.12	0.026
T*C	2.1	0.8	2.70	0.043

SE, standard error; Coeff, coefficient.

Table 4 lists the coefficients of the quadratic model for particle size and flow rate, respectively. For particle size, acid concentration (A) and its square term (A^2), and the interaction term between acid and its concentration (A*C) were found to be significant. Conversely, for flow rate, only the square terms of acid (A^2) and its concentration (C^2) and the interaction term between acid and concentration (A*C) were significant.

The ANOVA table of the analysis (Table 5) showed the quadratic model as significant for particle size. Likewise, for flow rate the quadratic model with the interaction terms were shown as significant.

The goodness of fit statistic was examined by the coefficient of determination (r^2), which indicates how much variation in the responses is explained by the quadratic model composed by the terms shown in Table 4. The higher the r^2, the better the data fits to the model and the better the model describes the relationship between the factors and the responses. Thus, about 95.13 % and 93.18 % of the experimental variances for particle size and flow rate, respectively, were explained by the quadratic model. The remaining experimental variation is attributed to random error and considered to be negligible.

Table 5: ANOVA table for particle size and flow rate of MCC II

Source	DF	SS coeff	Adjusted SS	Adjusted MS	F	p-value
Regression	9	20503.6	20503.6	2278.18	10.86	0.009
Linear	3	13357.2	2520.0	840	4.00	0.085
Square	3	5391.2	5343.7	1781.2	8.49	0.021
Interaction	3	1755.2	1755.2	585.1	2.79	0.149
Residual error	5	1049.1	1049.1	209.8	-	-
Lack-of-Fit	2	243.7	243.7	121.9	0.45	0.673
Pure error	3	805.3	805.3	268.4	-	-
Total	14	21552.7	-	-	-	-
S = 14.4851				r^2 = 0.9513		
Regression	9	351.5	351.5	39.06	7.55	0.019
Linear	3	153.1	18.2	6.05	1.17	0.408
Square	3	107.3	108.9	36.31	7.02	0.031
Interaction	3	91.1	91.1	30.37	5.87	0.043
Residual error	5	25.9	25.9	5.17	-	-
Lack-of-Fit	2	9.3	9.3	4.63	0.84	0.514
Pure error	3	16.6	16.6	5.53	-	-
Total	14	377.4	-	-	-	-
S = 2.2745				r^2 = 0.9315		

SS, standard error; MS, mean of squares; S, variance.

Further, these high r^2 values indicate that the quadratic models are a good predictor for particle size and flow rate, and the models describe very well the relationship between the three factors (acid type, concentration and hydrolysis time).

The quadratic models were validated by the lack of fit test. In this case, the goodness of fit statistical test evaluates whether the variation due to lack of fit of the model is small enough to be accepted as a negligible portion of the pure error. Thus, the corresponding null hypothesis (H_0) is that the lack of fit error is zero. Results indicate that *p*-value for the lack of fit was > 0.05, and thus, H_0 could not be rejected and the quadratic models were sufficient to accurately describe the observed variation in particle size and flow rate. Therefore, the experimental variations observed for these responses could be attributed to random errors (p = 0.673 and p= 0.514, for particle size and flow rate, respectively).

The quadratic models were used to predict the optimal reaction conditions according to the desired particle size of 100 µm and flow rate of 20 g/cc. In this case, two solutions were obtained. The first one gave a particle size

of 101 µm and a flow rate of 18 g/ cm^3 when hydrochloric acid is used for 3 h and at a 2.2 M concentration. The second solution gave a particle size of 102 µm and a flow rate of 18 g/cm^3 when sulfuric acid is employed at the same hydrolysis conditions. Conversely, it was not possible to find a solution when nitric acid is used for MCCII hydrolysis. The two predicted results were validated by conducting two runs at the optimized reaction settings. Therefore, the resulting particle size and flow rate for hydrochloric and sulfuric acids were 112 µm and 24.3 g/cm^3, and 96 µm and 17.2 g/cm^3, respectively.

The tableting properties of compacts made of spironolactone and MCCII treated at the different hydrolysis conditions is shown in Table 6. Since compacts were made at 0.1-0.15 porosity, their resulting tensile strengths exhibited a narrow range (2.2-2.4 MPa). Likewise, MCCII compacts showed a fast compact burst (disintegration times of 9-44.4 sec). It has been reported previously that the rapid compact disintegration of MCCII is due to its fast ability for water wicking. In this case, compact disintegration was not hindered by the presence of a 20% level of a poorly soluble drug such as spironolactone (0.028 mg/mL).

Table 6: Tableting properties of compacts made of MCCII and spironolactone (80:20 ratio)

Hydrolysis condition	Tensile strength (MPa)	Disintegration time (sec)	Weibull parameters			
	n=3	n=3	a	b	T_{80} (min)	r^2
HCl 3M 5h	2.2 (0.0)	13.0 (2.0)	7.34	0.86	17.9	0.9974
HNO_3 3M 3h	2.1 (0.1)	14.0 (1.0)	7.34	0.86	17.9	0.9973
HCl 5M 4h	2.2 (0.0)	12.0 (2.0)	23.50	1.00	33.1	0.9924
HNO_3 5M 4h	2.3 (0.0)	18.0 (2.0)	7.86	0.75	28.9	0.9895
H_2SO_4 1M 3h	2.2 (0.0)	13.7 (1.5)	12.36	0.92	26.3	0.9931
HCl 3M 3h	2.2 (0.1)	44.3 (6.1)	12.73	0.88	31.1	0.9905
H_2SO_4 3M 4h	2.4 (0.1)	9.0 (1.0)	19.10	1.00	30.1	0.9944
H_2SO_4 3M 4h	2.3 (0.0)	9.0 (1.0)	9.72	0.84	26.6	0.9887
H_2SO_4 3M 4h	2.2 (0.0)	12.3 (2.5)	6.09	0.71	25.3	0.9637
HNO_3 1M 4h	2.2 (0.0)	35.3 (7.5)	35.40	1.16	33.1	0.9939
H_2SO_4 1M 5h	2.3 (0.1)	17.7 (2.5)	10.35	0.86	26.5	0.9964
HCl 1M 4h	2.3 (0.0)	30.0 (5.0)	20.48	0.99	34.3	0.9914
H_2SO_4 5M 5h	2.3 (0.0)	17.7 (2.5)	9.30	0.79	30.6	0.9920
H_2SO_4 5M 3h	2.3 (0.1)	20.0 (2.5)	20.62	1.00	29.9	0.9940
HNO_3 3M 5h	2.3 (0.1)	32.7 (3.5)	14.60	0.97	25.7	0.9723
p-value	**0.215**	**0.447**	**0.91**			

The release properties of a drug from tablets depend on its solubility in the medium and the physicochemical properties of the polymer. Since MCCII is hydrophilic, its compacts could act as a non-swellable matrix which should not prevent drug release due to its rapid compact burst upon water wicking disrupting all the interparticle bonds. In order to compare the rapid release profiles, compacts of MCCII and spironolactone were made and the drug dissolution data were fitted to the general empirical equation described by Weibull using the Statgraphic software (v. 5, Warrenton, VA)[24].

$$F = 1 - exp^{\frac{[-(t)^b]}{a}} \qquad \text{Eqn. 2}$$

Where, "a" is the time scale of the process and "b" is a curve shape parameter. This shape could be either exponential (b= 1), sigmoid (b> 1) or parabolic (b <1). This model has been used in many types of dissolution profiles. Table 6 shows the "a" and "b" parameters and the resulting times to release 80% of spironolactone from compacts. Except for MCCII treated with 1M HNO_3 for 4h, in all cases "b" values were ≤ 1 indicating a change from exponential to a parabolic shape. The r^2 obtained from the Weibull model was > 0.9723 indicating a good fit of the data to this model.

However, this model has been widely criticized because its parameters are not related to the intrinsic dissolution rate of the drug[25]. In this case, the rate is determined by "a" and "b" altogether. Thus, for comparison purposes, only the predicted time to release 80% of the drug (t_{80}) is shown in Table 6.

Since compact tensile strength and compact porosity remained almost constant and compact disintegration time was fast (< 14 sec), variation of drug dissolution times cannot be attributed to the former factors, but the physical interaction between drug, release medium and MCCII particles.

CONCLUSION

This study demonstrated that wood cotton can be used to obtain MCCII for direct compression of drugs. Further, most of the tableting and powder properties did not depend on the hydrolysis conditions employed, except for particle size and flow rate. Further, the combined effect of particle size and bulk density was correlated to the degree of polymerization of MCCII. The typical rapid

disintegration properties of MCCII were not affected by the hydrolysis conditions employed. Further, dissolution times of spironolactone compacts were not affected by the acid-treated MCCII since this excipient always shows a rapid compact burst upon contact with water.

Acknowledgements: The authors acknowledge the staff of the drug pilot plant and Ana Giraldo for their help in the development of this project.

REFERENCES

1. Mohamed ES, Mohammad LH, Physical and mechanical properties of microcrystalline cellulose prepared from agricultural residues, Carbohydr Polym, 67, 2007, 1-10.
2. Williams RO, Sriwongjanya M, Barron MK, Compaction properties of microcrystalline cellulose using tableting indices, Drug Dev Ind Pharm, 23, 1997, 695-704
3. Kazakova EG, DeminVA, A new procedure for preparing microcrystalline cellulose, Russ J Appl Chem, 82, 2009, 496–499
4. Camacho F, Gonzalez P, Jurado E, Robles A, Microcrystalline-cellulose hydrolysis with concentrated sulphuric acid, J Chem Tech Biotechnol, 67, 1996, 350-356
5. El-Sakhawy M, Hassan ML, El-Sakhawy M, Hassan ML, Physical and mechanical properties of microcrystalline cellulose prepared from agricultural products, Carbohydr Polym, 67, 2007, 1-10
6. Landin M, Martinez-Pacheco R, Gomez-Amoza J, Souto C, Concheiro A, Rowe R, Influence of microcrystalline cellulose source and batch variation on the tabletting behaviour and stability of prednisone formulations, Int J Pharm, 91, 1993, 133-141
7. Rowe R, McKillop A, Bray D, The effect of batch and source variation on the crystallinity of microcrystalline cellulose, Int J Pharm, 101, 1994, 169-172
8. Araki J, Wada M, Kuga S, Okano T, Flow Properties of Microcrystalline Cellulose Suspension Prepared by Acid Treatment of Native Cellulose, Colloids Surf. Physicochem Eng Aspects, 142, 1998, 75-82
9. Brittain HG, Lewen G, Newman AW, Fiorelli K., Bogdanowich, S, Changes in Material Properties Accompanying the NF Identity Test for Microcrystalline Cellulose, Pharm Res, 10, 1993, 61-67
10. Das K, Ray D, Bandyopadhyay NR, Ghosh N, Mohanty AK, Misra M, Biodegradable nanocomposites from cellulosic, Cellulose, 16, 2009, 783-793
11. Bondeson D, Mathew A, Oksman K, Optimization of the isolation of nanocrystals from microcrystalline cellulose by acid hydrolysis, Cellulose, 13, 2006, 171-180
12. Ohwoavworhua FO, Adelakun TA, Okhamafe AO, Processing pharmaceutical grade microcrystalline cellulose from groundnut husk: Extraction methods and characterization, Int J Green Pharm, 3, 2009, 97-104.
13. Westermarck S, Juppo AM, Kervinena L, Yliruusi J, Microcrystalline cellulose and its microstructure in pharmaceutical processing, Eur J Pharm Biopharm, 48, 1999, 199-206.
14. Abeer MA, Zeinab HA, Atef AI, Mona TA, Characterization of microcrystalline cellulose prepared from lignocellulosic materials. Part II: Physicochemical properties, Carbohydr Polym, 38, 2011, 676-687
15. Maurer A, Fengel D, Gerd Wegener, Peter Glos, Parallel orientation of the molecular chains in cellulose I and II deriving from higher plants, HolzalsRohund Wekstoff, 50, 1992, 493-494.
16. Kumar V, Reus M, Yang D, Preparation, characterization, and tabletting properties of a new cellulose-based pharmaceutical aid, Int J Pharm, 235, 2002, 129-140.
17. Reus M, Kumar V, Evaluation of cellulose II powders as a potential multifunctional excipient in tablet formulations, Int J Pharm, 322, 2006, 31-35
18. Meyer V, editor. Annual Book of ASTM STM. Section 6. Paints Related Coatings and Aromatics, Six Edition, West Conshhocken, PA, USA, 2006, 345-350.
19. Pharmacopoeial Convention, "The United States Pharmacopoeia 32/National Formulary 29 (USP 32/NF29)," Washington, DC, 2005.
20. Fell JT and Newton JM, The tensile strength of lactose tablets, J Pharm Pharmacol 20, 1968, 657-758.
21. Klemm D, Philipp B, Heinze T, Heinze U, "Comprehensive Cellulose Chemistry: Functionalization of Cellulose," 2nd ed., John Wiley & sons, New York, 1998.
22. Kothari SH, Kumar V, Banker GS, Comparative evaluations of powder and mechanical properties of low crystallinity celluloses, microcrystalline celluloses, and powdered celluloses, Int J Pharm, 232, 2002, 69-80.
23. Carrillo F, Colom X, Sunol JJ, Saurina J, Structural FT-IR analysis and thermal characterization of lyocel and viscose-type fibers, Eur Polym J, 40, 2004, 229-234.
24. Weibull W, Dissolution of fludrocortisone from phospholipid coprecipitates, J Applied Mech, 18, 1951, 293-297.
25. Pedersen PV and Myrick JW, Versatile kinetic approach to analysis of dissolution data, J Pharm Sci, 67, 1978, 1450-1455.

****